Structural and electronic properties of pentagon-heptagon pair defects in carbon nanotubes

J.-C. Charlier*
Unité de Physico-Chimie et de Physique des Matériaux, Université Catholique de Louvain, 1 Place Croix du Sud, B-1348 Louvain-la-Neuve, Belgium

T. W. Ebbesen
NEC Research Institute, 4 Independence Way, Princeton, New Jersey 08540

Ph. Lambin
Institute for Studies in Interface Sciences, Facultés Universitaires Notre-Dame de la Paix, 61 Rue de Bruxelles, B-5000 Namur, Belgium

(Received 26 September 1995)

General features of the energetics and electronic states of carbon nanotubes, containing pentagon-heptagon pair (5/7) topological defects in the hexagonal network of the zigzag configuration, are investigated within simple tight-binding models. This 5/7 pair defect on the nanotube structure is not only responsible for a change in nanotube diameter, but also governs the electronic behavior around the Fermi level. Furthermore, nanotubes having different helicities and different electronic properties can be connected using such a pair. Various configurations including one, two, and three 5/7 pairs are explored in order to understand the influence of several defects on the electronic properties of the system. Topological aspects associated with the presence of 5/7 pair defects in armchair and chiral nanotubes are also discussed.

I. INTRODUCTION

Recently, experimental observations have shown that carbon nanotubes are rarely as perfect as they were once thought to be.[1,2] The possible defects structures can be classified into three general groups: topological (introduction of ring types other than hexagons), rehybridization (ability of carbon atom to hybridize between sp^2 and sp^3), and incomplete bonding defects (vacancies, dislocations, etc.).

In the present study, we are interested in introducing pentagon-heptagon (5/7) pairs in the cylindrical hexagonal network of the carbon nanotube (first-group defects).[3,4] In the absence of other cycles than hexagon rings, Euler's theorem imposes the inclusion of 12 pentagons in the hexagonal network to close the structure. However, the addition of one heptagon in the cylindrical surface of the nanotube will require the presence of 13 pentagons to close the structure as the heptagon and the pentagon induce opposite 60° disclinations in the surface. When the pentagon is attached to the heptagon as in the aniline structure, it only creates topological changes (but no net disclination) which can be treated as a single local defect. Such a pair will create only a small local deformation in the width of the nanotube. It may also generate a small change in the helicity, depending on its orientation in the hexagonal network.[5,6] So their presence is hard to detect experimentally, but observations of carbon tubules becoming gradually thicker and thicker can be attributed to a very large number of these 5/7 pair defects accidently aligned.[1] The existence of these nanotubes indicates that such pairs are probably common in these cylindrical structures but they normally go undetected because they cancel each other out when randomly aligned.[1]

The electronic structure of a perfect nanotube is known to be either metallic or semiconducting, depending on the diameter and chirality,[7–9] which can uniquely be determined by the chiral vector (n,m), where n and m are integers.[9] A general rule can be derived: metallic or semiconducting nanotubes are obtained whether or not $n-m$ is a multiple of 3, neglecting the small gap due to the effect of curvature.[10] It is clear that the presence of isolated pentagon or heptagon defects significantly perturbs the electronic properties of the hexagonal network.[11] Recent calculations, showing the influence of these defects on the electronic structure, have also been perfomed on helically coiled[12] and bent[13] nanotubes where *isolated* pentagons and heptagons are incorporated at opposite sides of the honeycomb lattice to form the helical structure.[5] However, a pentagon-heptagon pair defect can also be incorporated in a straight nanotube, allowing the connection of two cylindrical straight portions with different diameters and, possibly, chiralities, leading to the design of metal-semiconductor, metal-metal, or semiconductor-semiconductor devices.

The electronic structure is also affected, although only fairly locally, by the tip structure, which could introduce some topological defects such as pentagons. In view of the large aspect ratio of nanotubes (100 to 1000), the main body of the tube will remain unaffected. Some localized states, associated with the presence of pentagons in the tip structure, could appear in the region close to the Fermi energy, and thus, affect the electronic properties of the global system. However, the topology of the cap is still a matter of controversy, and will be the subject of another independent study.[14] The 5/7 pair defects we are interested in here appear to occur at a non-negligeable frequency (as much as one every three nanometers[2]) in which case the electronic structure of the entire tube would be much more severely affected.

In this paper, we examine the structural and electronic properties of zigzag nanotubes $(n,0)$ containing one, two,

and three pentagon-heptagon pair defects. Different configurations for the 5/7 distribution are investigated, and our results show that topological structure where defects are aligned along the cylindrical axis of the tube, are found to be more stable after tight-binding molecular-dynamics relaxation than geometries with defects distributed along the circumference of the tube. The densities of states (DOS's) of these systems are computed by a tight-binding Hamltonian, and present, in essentially each structure, interesting localized states per 5/7 defect, associated with different particular sites in the five- and seven-membered rings, which govern the electronic behavior around the Fermi level. Finally, general features on the influence of these 5/7 pair defects on the properties and topology of armchair and chiral nanotubes are presented.

II. ATOMIC STRUCTURE

In this section, we investigate the energetics of different distributions of 5/7 pair defects on the cylindrical surface of zigzag nanotubes $(n,0)$. No calculation was performed for armchair nanotube (n,n) including 5/7 defects, as such topology favors the presence of two opposite 5/7 in order to not disrupt too much the hexagonal network, as it is the case for a single 5/7 defect (see Sec. IV). The perturbed nanotube is composed of a starting straight nanotube portion (12,0), which is connected by a joint, containing one, two, or three 5/7 defects, to a (11,0), (10,0), or (9,0) cylindrical portion, respectively. Six different joints are investigated: (Ia) (12,0)-(11,0) with a single 5/7 defect, (IIa) (12,0)-(10,0) with two 5/7 defects positioned at opposite sides of the conical surface, (IIb) (12,0)-(10,0) with two 5/7 defects aligned along the tube axis, (IIc) (12,0)-(10,0) with two 5/7 defects side-by-side, leading, after structural relaxation, to a peculiar 5/6/7 topological defect, (IIIa) (12,0)-(9,0) with three 5/7 defects positioned as far as possible from each other on the conical surface (trigonal arrangement), and (IIIb) (12,0)-(9,0) with three 5/7 defects aligned along the tube axis, as illustrated in Fig. 1.

These systems are selected because their electronic properties are expected to differ radically. Indeed, whereas the (12,0)-(9,0) system connects two metallic nanotubes, the two others are prototypes for metal-semiconductor junction. For reasons of simplicity, each aniline defect is aligned with the tubule axis, leading the two straight portions of the tube to be achiral (zigzag type). For example, a 60° rotation of a 5/7 defect would have connected the achiral (12,0) nanotube to a chiral (11,1) one. A more complete description of the topology of these 5/7 pairs in the hexagonal network will be presented in Sec. IV.

The different atomic structures of the joint connecting the two nanotubes and containing the 5/7 pair defects, either distributed along the circumference or aligned along the axis of the tube, are relaxed on the computer using tight-binding molecular dynamics, as proposed in a recent efficient linear scaling algorithm.[15] A suitable repulsive potential for carbon, which is known to accurately describe linear chains (twofold), graphite (threefold), and diamond (fourfold) structures,[16] is used to stabilize the structure of the nanotube. In each case, the joint, including three unperturbed belts of hexagons, is connected to its opposite image in a unidimensional periodic unit cell. The different unit cells contain, respectively, 230 (Ia), 220 (IIa), 352 (IIb), 264 (IIc), 210 (IIIa), and 462 (IIIb) carbon atoms. The one-dimensional structure is also reproduced periodically in the other two directions, with a 10-Å interspace between the carbon systems. This distance is large enough to prevent a significant interaction between the nanotubes.

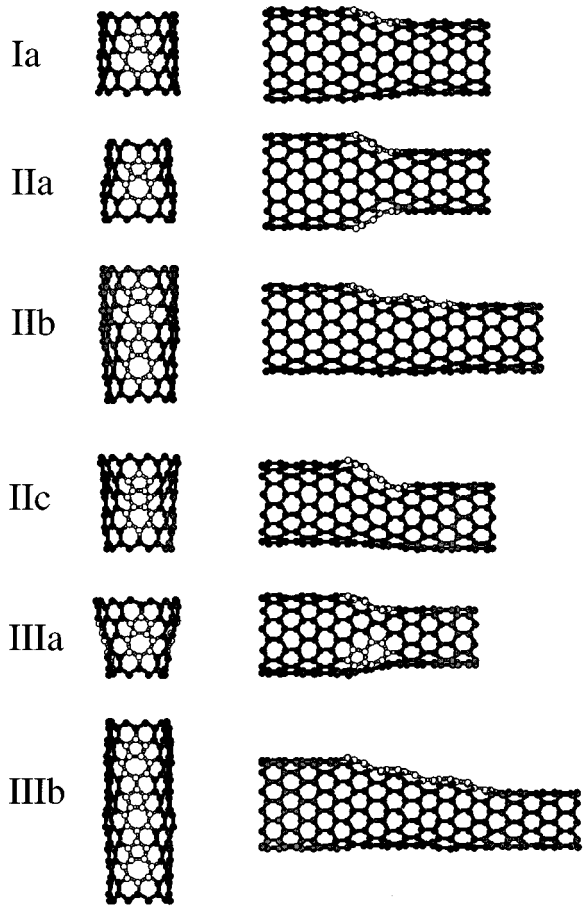

FIG. 1. Relaxed structures of different joints connecting two zigzag nanotubes: (12,0), and (11,0) (I: single 5/7 defect), (10,0) (II: double 5/7 defects), (9,0) (III: triple 5/7 defects), respectively. The 5/7 pair defects are either distributed around the circumference of the tube (a), aligned along the cylindrical axis (b), or transformed into another defect: as 5/6/7 defect (IIc). The pentagon and heptagon rings, responsible for the change in nanotube diameter, are visualized in white, while the rest of the joint is in grey. The left-hand side of the figure shows the top of the structure which includes the 5/7 pair defects. The right-hand side is a projection of the structure, elongated by a few belts of hexagons, on a symmetry plane passing through the 5/7 defect(s).

The energy values relative to different numbers of 5/7 defects perturbing the cylindrical structure of the nanotube are summarized in Table I. The results correspond to total-energy calculations of the defected joints, after a relaxation of the structure from 100 K to 0 K during 1 ps, which are subtracted by the amount of total energy of the ideal unperturbed cylindrical nanotube, in order to present the effective energetical contribution of the defect(s). The optimized structures for the different joints are illustrated in Fig. 1.

These results show that 5/7 pair defects are more stable

TABLE I. Increase in energy (in eV/atom) for the different joints investigated in the present study relative to the pure cylindrical case. The (c) column is for the peculiar case of a 5/6/7 defect.

Energy per atom (eV/atom)	(a) 5/7 defects distributed around the axis	(b) 5/7 defects aligned along the axis	(c) Peculiar defects
(I) single 5/7 defect	0.132		
(II) two 5/7 defects	0.258	0.249	0.208
(III) three 5/7 defects	0.405	0.291	

when aligned along the nanotube axis rather than placed around the cylindrical circumference. In addition, in the case where two 5/7 pair defects are placed close to each other, the relaxation of the structure directly creates a new stable default constituted by a pentagon and a heptagon, isolated by a distorted hexagonal ring (IIc). The energy associated with this 5/6/7 defect shows that the incorporation of an isolated pentagon and heptagon is less stable than the introduction of a single 5/7 pair defect (+ 0.076 eV/atom). The creation of a hexagon ring separating pentagon and heptagon is, however, an interesting way to relax two side-by-side 5/7 defects.

Table II summarizes the averaged bond lengths in the pentagon(s), heptagon(s), and hexagons of the different joints. In nearly each structure, the average bond length in the pentagon(s) [heptagon(s)] is found to be slightly longer (shorter or nearly equivalent) than the one of the hexagons. For the pentagonal case, this could be explained by analogy with the fullerenes. In addition, the pentagon shape is essentially found to be planar with a very small distortion, although the heptagon is boat shaped in order to reduce its bond angles in the range 124° – 126°, and to suitably accomodate the local negative curvature of the carbon network. The purely cylindrical shape of the nanotube is also perturbed by the presence of these 5/7 pair defects. The belt of hexagons containing the pentagon is found to be elliptical, with the long axis passing through the perturbing ring; while for the belt containing the heptagon, the section of the nanotube is elongated in the perpendicular direction. The ratio between the two axes of the two ellipses of the joint are 0.81 (5) and 0.90 (7) for a single 5/7 defect (Ia), and 0.66 (5) and 0.85 (7) for two opposite-side 5/7 defects (IIa). This process can be viewed as streching by the pentagon, and reciprocally, flattening by the heptagon of the circular section of the tube. A few belts of hexagons away from the 5/7 defect, the cylindrical shape of the nanotube reappears.

III. ELECTRONIC PROPERTIES

The electronic properties of the previously described systems are explored by application of the recursion method[17] within a tight-binding description of the carbon π bands. Only first-neighbor C-C interactions are considered, with the two-center hopping integral $V_{pp\pi}$ set at -3.1 eV.[18] The other tight-binding terms are neglected in this approach as well as the hybridization due to the curvature of both joint and tube, the effect of which is considered to be sufficiently small even for the smallest nanotube diameter.[8]

For each structure, the joint is connected to two very long ($\sim$ semi-infinite, $\pm$ 5000 carbon atoms each) nanotubes, the diameters of which correspond to the ones of both ends of the joint, as described in the previous section. The nanotubes are taken long enough to avoid border effects, which could come from the dangling π bonds at the two edges of the nanotubes and give rise to edge states at the Fermi level. The recursion technique, used in the present study, allows the calculation of the density of states, directly related to the topology of the carbon network (how carbon atoms are connected), and not to the detailed relaxation of the joint structure. In addition, this scheme does not recur to the Bloch's theorem, and consequently, the calculation is performed on the joint without any periodic boundary condition along the direction parallel to the axis of the nanotube. Bloch's theorem would have imposed the use of an artificial finite model such as the supercell containing the 5/7 defect(s) and its (their) opposite image(s) as in Sec. II, which would have certainly perturbed the electronic properties associated with the 5/7 pair defect(s) of the joint.

The electronic properties of the metal-semiconductor (12,0)$-$(11,0) junction (case Ia) are illustrated in Fig. 2. The left part of this figure shows the π densities of states of the isolated (12,0) and (11,0) nanotubes. The Fermi energy ϵ_F coincides with the atomic π level, taken as zero of

TABLE II. Atomic structure analysis of the bond lengths for the different joints investigated in the present study. The bond lengths are averaged over the pentagon(s), the heptagon(s), and the hexagons of the respective joints. The averaged angles for the boat-shaped heptagons are also given.

Atomic structure of the joints	(a) Bond length in pentagon(s) (Å)	(b) Bond length in heptagon(s) (Å)	(c) Bond length in hexagons (Å)
(Ia) single 5/7 defect	1.439	1.433 (126.5)	1.420
(IIa) two distributed 5/7 defects	1.434	1.400 (125.7)	1.414
(IIb) two aligned 5/7 defects	1.465	1.417 (125.7)	1.418
(IIc) single 5/6/7 defect	1.482	1.400 (124.2)	1.421
(IIIa) three distributed 5/7 defects	1.457	1.442 (125.1)	1.436
(IIIb) three aligned 5/7 defects	1.447	1.423 (125.5)	1.420

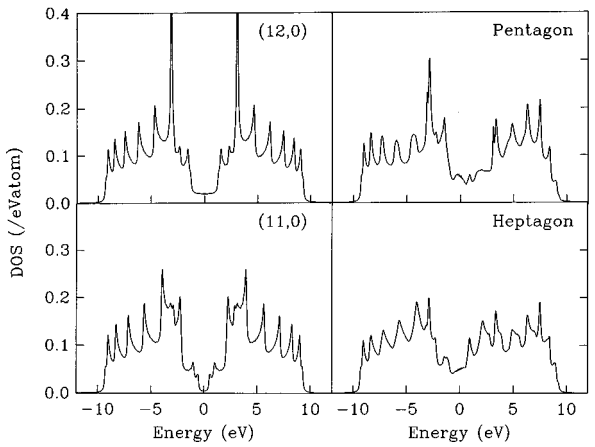

FIG. 2. Densities of π electron states in the isolated (12,0)-metallic and (11,0)-semiconducting nanotubes of the Ia case, and local densities of states on the five- and seven-membered rings of the single 5/7 pair defect, are illustrated in the left and right parts of the figure, respectively. All these curves were obtained from the recursion method to 150 levels in the continued fraction expansion of the Green function, corresponding to 300 exact moments of the DOS. A small imaginary part (0.02 eV) was added to the energy in order to make the continued fraction convergent.

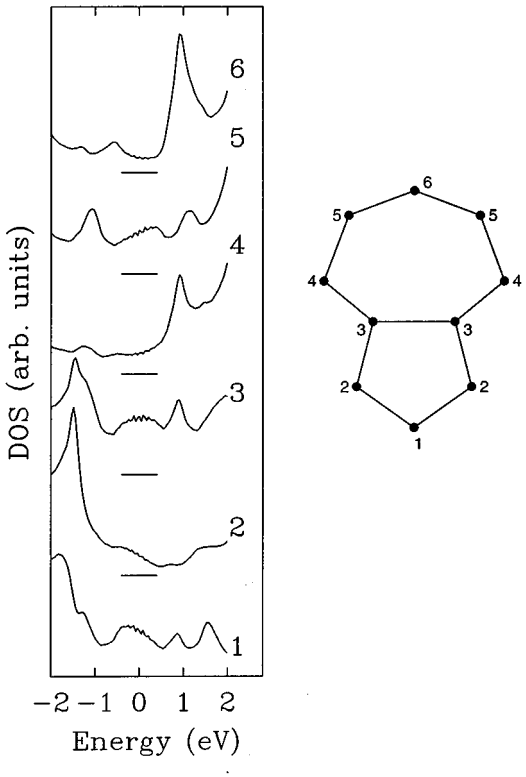

FIG. 3. Local densities of states averaged on different sites of the two five- and seven-membered rings of the single 5/7 pair defect. The curves are labeled 1 to 6, corresponding to the atomic sites in the right-hand-side representation of the 5/7 defect. The left-hand panel details the densities of states in a narrow interval around the Fermi level at zero energy. The horizontal bars indicate the zero-density levels.

energy. The energies of the eigenstates are within $|E| \leqslant 3 \times V_{pp\pi}$, which is consistent with three C-C bonds from each carbon atom. The (12,0) nanotube is metallic, with a density of states at ϵ_F, around 0.026 state/eV/atom. As shown in Fig. 2, the DOS of this nanotube presents a plateau which extends 1.2 eV on both sides of the Fermi level, indicating the existence of one-dimensional metallic energy bands. The (11,0) nanotube is a semiconductor with a band gap of 0.8 eV. Both isolated nanotube densities of states not only present the two-dimensional van Hove singularities of graphite at $E = \pm V_{pp\pi}$ ($\pm$ 3.1 eV), but also many sharp peaks coming from the inverse square-root divergence ($1/\sqrt{E}$) of the spectra of the one-dimensional (1D) bands. These singularities are due to the quantization of the 1D energy bands in the circumferential direction.

The right-hand side of Fig. 2 shows the DOS's averaged over the five and seven sites of the pentagon and heptagon of the 5/7 defect. The electron-hole symmetry of the density of states is destroyed at the two defects, as they are odd-membered rings.[11] As a consequence, the corresponding local DOS does not integrate exactly to 1 at the Fermi level. There is a slight excess of electrons on the pentagonal ring and a small electron deficit on the heptagon, agreeing with previous calculations on bent nanotubes.[13] Our results are in accordance with the general fact that, in a planar hexagonal network, even-membered rings are neutral, five-memberd rings are attractive, and seven-membered rings are repulsive of electrons.[11]

Of special interest in the electronic states of this system is the emergence of two resonant states near the Fermi level, as presented in Fig. 3. That is to say, a clear peak structure appears for sites 2 of the pentagon, at an energy slightly lower than ε_F (at about -1.5 eV), and another peak appears at sites 4 and 6 of the heptagons, at an energy slighly above ε_F (at about 1.0 eV). Contributions from the sharing 5/7 carbon bond (sites 3), although smaller, are also visible. The fact that the former peak is caused by the pentagon and the latter by the heptagon is in opposition to recent tight-binding calculation performed on a 5/7 pair defect in a graphite sheet.[11] As site 2 is nearer to the seven-membered ring than site 1, and site 4 is nearer the five-membered ring than site 5, these peaks are preferentially appearing at sites 2 and 4, and not at sites 1, and 5, respectively, as mentioned in Tamura *et al.*[11]

Analyzing the whole metallic-semiconducting junction of case Ia, Fig. 4 illustrates how the density of states around ε_F varies from section to section along the (12,0)$-$(11,0) connection. When moving upwards from the starting ring (1) to the first ring of the junction (6), the density of states oscillates, with the period of the lattice, around the value of the plateau, calculated for the (12,0)-isolated nanotube. The DOS oscillations take place over a large range distance in front of the junction. When continuing upwards, away from the junction (rings 13 to 18), the local DOS again alternates between low and somewhat higher values, while vanishing progressively. The band gap does not settle right away because the junction is a continuous transition between the two segments of straight nanotube. It requires a distance of about $\pm$ 20 Å below the joint to recover completely the semiconductor behavior.

Attention is now given to the multiple 5/7 pair defects systems. The six junctions, investigated in the previous

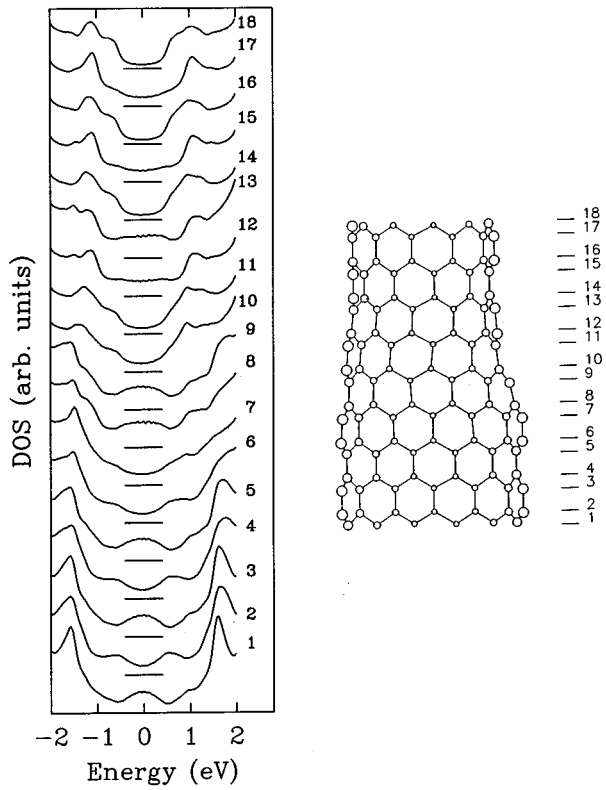

FIG. 4. Optimized atomic structure (right) and π-electron density of states of the (12,0)-(11,0) connection. In a narrow interval around the Fermi level (zero energy), the curves, labeled 1 to 18, represent the densities of states averaged over 12 or 11 atoms at the sections indicated by the corresponding letters in the right-hand-side projection of the structure. The horizontal bars indicate the zero-density levels.

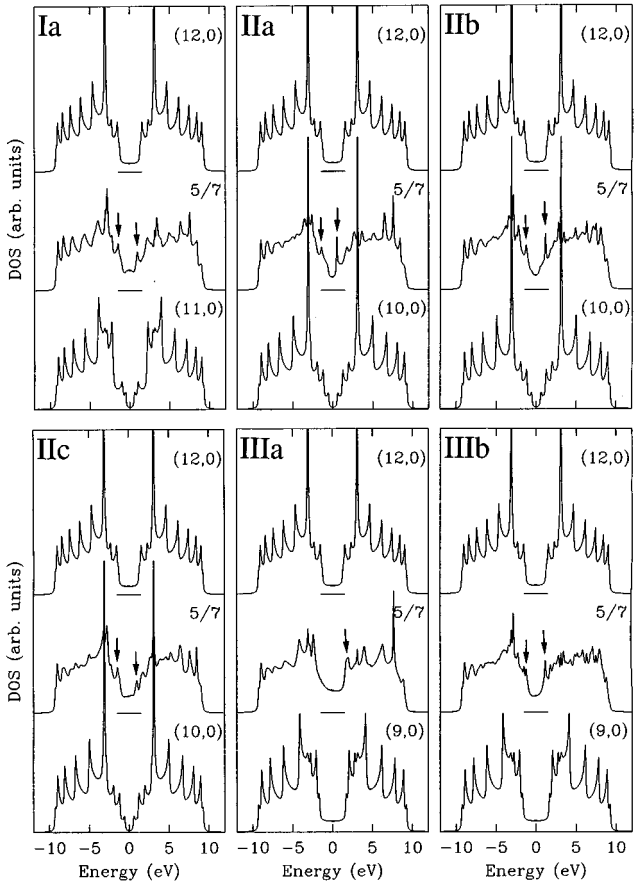

FIG. 5. Densities of π electron states in the isolated (12,0), (11,0), (10,0), and (9,0) nanotubes of the six cases investigated in the present study, as labeled in Fig. 1. In each case, the two DOS's of the isolated nanotubes connecting the respective junctions, are separated by the local density of states averaged over the number of 5/7 pair defects present in the joint. Main resonant states associated with the 5/7 pairs are shown by arrows. The horizontal bars indicate the zero-density levels.

section, are presented in Fig. 5, illustrating the π densities of states of the two nanotubes connected by the respective junctions, and separated by the local density of states averaged over the 5/7 pair defects included in the joint. In nearly every structure, the presence of resonant states, coming from the pentagonal and heptagonal atomic sites, is clearly visible. One sharp peak below and above the Fermi level can be associated with one 5/7 pair defect. However, sometimes the peaks, coming from different defects, are situated exactly at the same place. This explains why the number of sharp peaks in the Fermi region is not twice the number of defects present in the respective joints. In the peculiar cases where 5/7 pair defects are aligned along the direction of the tube (IIb and IIIb), the main contribution comes from the first pair defect, and vanishes for the other 5/7.

IV. DISCUSSION

In the preceding sections, we investigate the structural and electronic properties of zigzag nanotubes including 5/7 pair defects parallel to the axis of the cylindrical carbon honeycomb network. These cases (Ia, IIa, IIb, IIc, IIIa, and IIIb) are particular topological defect structures among various structural possibilities created by introducing a 5/7 pair defect in the nanotube configuration, as explained below.

The orientations of the hexagonal network and 5/7 defect, relative to each other and to the nanotube axis, determine what changes the defect introduces in the tube. If we consider the orientation of the 5/7 pair defect to be the axis of symmetry passing through the middle of the five- and seven-membered rings, then certain general features can be formulated.

(i) Only in zigzag tube $(n,0)$, can the 5/7 pair defect be exactly aligned with the tube axis. There will be a change in diameter but no change in the helicity (the tube remains achiral on both sides of the defect). So only this relative orientation makes possible an achiral to achiral connection between two segments of different tubes.

(ii) When the 5/7 pair defect is perpendicular to the tube axis, in such a way that the mirror plane passes through the axis of the 5/7 defect, a unique case is obtained.[19] On each side of the defect, the tube is chiral but they are mirror images, i.e. enantiomers, but the circumference remains unchanged. The tube will be slightly bent around the defect.

(iii) In any other orientation, the 5/7 pair defect and the hexagonal network will affect both the diameter (circumference) of the tube and the chirality. In such cases transitions from achiral to chiral tube are possible. The change in chirality is only one step per turn per defect.

Case (ii) is unique in that, starting from the tube defect, the spirals in the hexagonal network are opposite and mirror images of each other. This means that $(n,n-1)$ can be connected to a $(n,1-n)$ tube through such an arrangement. However, if we start with an armchair tube (n,n) on one side, then add a 5/7 pair defect, a $(n+2,n-2)$ chiral tube will be obtained. In this case the 5/7 pair defect axis is not exactly perpendicular. It should be added that the enantiomer obtained depends on the direction of the 5/7 pair defect either $5\rightarrow7$ or $7\rightarrow5$ relative to the achiral tube. By analogy with the chemical nomenclature, either a clockwise (r, rectus) or counterclockwise (s, sinister) tube will be formed.

As the calculations show here, the addition of 5/7 pair defects to nanotubes allows for interesting connections between tubes having different properties.[5,6,11–13] However, the most important issue is, perhaps, their natural presence in raw nanotubes since they will seriously affect the electronic properties that are measured, and produced unexpected results.[1] In essentially all the configurations invesigated in the present study, the density of states reveals resonant states, associated with different peculiar sites in the five- and seven-membered rings. The observation of resonant states (sharp peaks) in the density of states of nanotube bundles, close to the Fermi level, would be a proof of their existence. Energetic results show that topological structure where defects are aligned along the cylindrical axis of the tube is found to be more stable after tight-binding molecular-dynamics relaxation than geometries with defects distributed along the circumference of the tube. In analyzing the effect of 5/7 pair defects on large fullerenes, Saito *et al.*[20] pointed out that a 5/7 pair defect can move in the hexagonal network and annihilate with another 5/7 pair when these are oriented in opposite directions. So we can expect that a significant fraction of 5/7 pairs and other defects will anneal away at high temperatures. Indeed, annealing nanotubes at high temperatures (ca. 3000 K) has a strong effect on the conduction-electron spin-resonance properties.[2] It might be not possible to eliminate all the 5/7 pair defects by annealing but it should improve the consistency and quality of the measured results. Therefore, studying local changes of the electronic structure induced by topological defect is very important in trying to understand the characteristics of closed cylindrical graphite surfaces.

ACKNOWLEDGMENTS

The authors would like to thank Dr. S. Goedecker for the availability of the tight-binding molecular-dynamics code, and acknowledge informative discussion with Dr. X. Gonze, Dr. J.-M. Beuken, Ph. Ghosez, and G.-M. Rignanese in the early stages of the present project. Two of the authors (J.C.C. and Ph.L.) are grateful to the National Fund for Scientific Research (FNRS) of Belgium for financial support. This paper presents research results of the Belgian Program on Interuniversity Attraction Poles initiated by the Belgian State–Prime Minister's Office–Science Policy Programming. We also aknowledge the use of the RS 6000 work stations and the Namur Scientific Computing Facility (Namur-SCF), which are common projects between IBM-Belgium and, respectively, the Catholic University of Louvain (UCL-PCPM) and the Facultés Universitaires Notre-Dame de la Paix (FUNDP-LPMPS).

*Present address: Institut Romand de Recherche Numérique en Physique des Matériaux (IRRMA), Ecole Polytechnique Fédérale de Lausanne (EPFL), INR–Ecublens, CH-1015 Lausanne, Switzerland.

[1] T.W. Ebbesen and T. Takada, Carbon **33**, 973 (1995).
[2] M. Kosaka, T.W. Ebbesen, H. Hiura, and K. Tanigaki, Chem. Phys. Lett. **233**, 47 (1995).
[3] S. Iijima, P.M. Ajayan, and T. Ichihashi, Phys. Rev. Lett. **69**, 3100 (1992).
[4] S. Iijima, T. Ichihashi, and Y. Ando, Nature **356**, 776 (1992).
[5] B.I. Dunlap, Phys. Rev. B **46**, 1933 (1992).
[6] B.I. Dunlap, Phys. Rev. B **49**, 5643 (1994).
[7] J.W. Mintmire, B.I. Dunlap, and C.T. White, Phys. Rev. Lett. **68**, 631 (1992).
[8] R. Saito, M. Fujita, G. Dresselhaus, and M.S. Dresselhaus, Phys. Rev. B **46**, 1804 (1992).
[9] N. Hamada, S.-I. Sawada, and A. Oshiyama, Phys. Rev. Lett. **68**, 1579 (1992).
[10] R. Saito, M. Fujita, G. Dresselhaus, and M.S. Dresselhaus, Appl. Phys. Lett. **60**, 2204 (1992).
[11] R. Tamura and M. Tsukada, Phys. Rev. B **49**, 7697 (1994).
[12] K. Akagi, R. Tamura, and M. Tsukada, Phys. Rev. Lett. **74**, 2307 (1995).
[13] Ph. Lambin, A. Fonseca, J.-P. Vigneron, J.B. Nagy, and A.A. Lucas, Chem. Phys. Lett. (to be published).
[14] J.-C. Charlier, A. de Vita, and R. Car (unpublished).
[15] S. Goedecker and L. Colombo, Phys. Rev. Lett. **73**, 122 (1994).
[16] C.H. Xu, C.Z. Wang, C.T. Chan, and K.M. Ho, J. Phys. Condens. Matter **4**, 6047 (1992).
[17] R. Haydock, V. Heine, and M.J. Kelly, J. Phys. C **8**, 2591 (1975).
[18] This value is $\sim$1.2 times that commonly accepted for C_{60} on the grounds of the local-density approximation, as the latter underestimates the $V_{pp\pi}$ parameter of graphite by about 20%. See J.-C. Charlier, X. Gonze, and J.-P. Michenaud, Phys. Rev. B **43**, 4579 (1991).
[19] A. Major, N. Taylor, A. Lawrence, N. Rivier, and J.F. Sadoc, Philos. Mag. B **55**, 507 (1987).
[20] R. Saito, G. Dresselhaus, and M.S. Dresselhaus, Chem. Phys. Lett. **195**, 537 (1992).